ICES Journal of Marine Science Advance Access published April 7, 2009

Modelling and simulations of the migration of pelagic fish

Alethea Barbaro, Baldvin Einarsson, Björn Birnir, Sven Sigurðsson, Héðinn Valdimarsson, Ólafur Karvel Pálsson, Sveinn Sveinbjörnsson, and Þorsteinn Sigurðsson

Barbaro, A., Einarsson, B., Birnir, B., Sigurðsson, S., Valdimarsson, H., Pálsson, Ó. K., Sveinbjörnsson, S., and Sigurðsson, Þ. 2009. Modelling and simulations of the migration of pelagic fish. – ICES Journal of Marine Science, 66: 00–00.

We applied an interacting particle model to the Icelandic capelin stock to reproduce the spawning migration route for three different years, successfully predicting the route for 2008. Using available temperature data and approximated currents, and without using artificial forcing terms or a homing instinct, our model was able to reproduce the observed migration routes from all 3 years. By a sensitivity analysis, we identified oceanic temperature and the balance between the influence of interaction among particles and the particles' response to temperature as the control parameters most significant in determining the migration route. One significant contribution of this paper is the inclusion of orders of magnitude more particles than similar models, which affects the global behaviour of the model by propagating information about surrounding temperature through the school more efficiently. To maintain the same dynamics between different simulations, we argue a linear relationship between the time-step, radii of interactions, and the spatial resolution, and we argue that these scale as $N^{-1/2}$, where N is the number of particles.

Keywords: collective motion, fish migration, Icelandic capelin, interacting particle model, *Mallotus villosus*.

Received 17 June 2008; accepted 4 February 2009.

A. Barbaro, B. Einarsson, and B. Birnir: Department of Mathematics, South Hall, University of California, Santa Barbara, CA 93106-3080, USA. B. Einarsson and B. Birnir: Faculty of Physical Sciences, University of Iceland, Hjarðarhaga 2-6, IS-101 Reykjavík, Iceland. S. Sigurðsson: Faculty of Industrial Engineering, Mechanical Engineering and Computer Science, University of Iceland, Hjarðarhaga 2-6, IS-101 Reykjavík, Iceland. B. Einarsson and B. Birnir: Center for Complex and Nonlinear Science, 6513 South Hall, University of California, Santa Barbara, CA 93106, USA. H. Valdimarsson, Ó. K. Pálsson, S. Sveinbjörnsson, and Þ. Sigurðsson: Marine Research Institute of Iceland, Skúlagötu 4, IS-121, Reykjavík, Iceland. Correspondence to B. Einarsson: tel:+354 692 9493; fax:+354 525 4632; e-mail: baldvine@hi.is.

Introduction

Capelin (*Mallotus villosus*) is a pelagic species which, like the herring (*Clupea harengus*), covers several hundred kilometres in its migration between feeding and spawning grounds (Vilhjálmsson, 1994, 2002; Misund *et al.*, 1998; Vilhjálmsson and Carscadden, 2002). In this paper, we focus on the stock inhabiting the Iceland Sea, hereafter referred to as the Icelandic capelin. Its role in the ecosystem of the Icelandic waters is highly significant, bringing large amounts of biomass from the Arctic to more southerly latitudes. Capelin is a vital part of the diet of fish species such as cod (*Gadus morhua*; Magnússon and Pálsson, 1991; Magnússon and Aspelund, 1997). Capelin catches are exported or processed into fishmeal and oils, and in recent years, the Icelandic fishing industry has relied on its value. However, the size of the stock has been diminishing, and much research effort has been put into stock estimation. It is therefore of importance to be able to model the whereabouts of Icelandic capelin to control catches. A brief account of pertinent details of this species is discussed here, but the interested reader is referred to Vilhjálmsson, (1994), who provides extensive details of the stock and its life cycle.

Icelandic capelin spend the first 2–3 years of their life in waters north of Iceland, along the edge of the continental shelf. When they approach maturity, usually either during spring of its second or third year, they undertake an extensive migration, herein referred to as the feeding migration, to the plankton-rich waters of the Iceland Sea as far north as the island of Jan Mayen. There, zooplankton is plentiful, and they feed on the vernal phytoplankton bloom in the region. The maturing capelin eat these zooplankton and grow extensively. In October and November, fully grown capelin return to the waters northwest and north of Iceland. In January, this portion of the stock undertakes a spawning migration around Iceland to the southern and western coasts. The spawning migration generally approaches along the continental shelf edge to the northeast and east of Iceland. However, in some years, a portion of the stock migrates against the coastal current and takes a westerly route to the spawning grounds. The capelin spawn in February/March then die, leaving the eggs to hatch and the larvae to drift with the coastal currents to the continental shelf waters north of Iceland and to begin the cycle again. The migrations of capelin are seasonal and vary by year, so it is clear that the environment has a significant impact on the migration pattern (Vilhjálmsson, 1994, 2002; Carscadden *et al.*, 1997).

A separate capelin stock resides in the Barents Sea, north of the coast of Norway and Russia. That stock has been widely studied and exhibits similar migration patterns between feeding and spawning grounds (Gjøsæter, 1998; Gjøsæter *et al.*, 1998). Much effort has been put into modelling that stock (Reed and Balchen,

1982; Fiksen *et al.*, 1995; Huse *et al.*, 1999, 2004; Huse, 2001; Sigurðsson *et al.*, 2002; Magnússon *et al.*, 2004a). However, the Barents Sea migration route differs significantly from the Icelandic one, because it contains no islands or other obstacles.

Previous models of the migratory behaviour of capelin use some sort of attraction towards the feeding or spawning grounds (Sigurðsson *et al.*, 2002; Hubbard *et al.*, 2004; Magnússon *et al.*, 2004a, b, 2005). Promising results for the Barents Sea stock were presented by Huse *et al.* (2004) using only environmental factors, but with some discrepancies between predictions and observations. Here, we use an interacting particle model based on the work of Hubbard *et al.* (2004) and Magnússon *et al.* (2004b). A notable difference between our model and previous models of capelin migration is the absence of an artificial forcing term. Also, the architecture of our code allows us to run the simulation with tens of thousands of particles, a significant improvement over previous models.

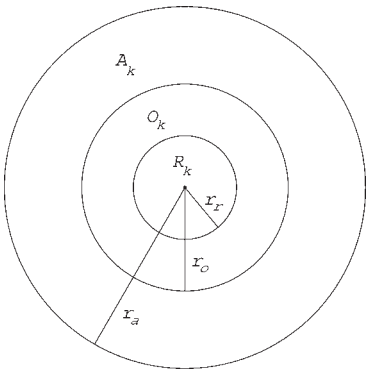

Figure 1. Zones of interaction (sensory zones) of particle k. A_k is its zone of attraction, O_k its zone of orientation, and R_k its zone of repulsion. These zones have radii r_a, r_o, and r_r, respectively.

Material and methods

Model outline

We describe the model using the Overview, Design concepts, and Details protocol defined in Grimm *et al.* (2006). Its main purpose is to investigate the extent to which migration patterns of capelin can be explained by the interaction between movement towards a preferred temperature, which may depend on age and maturity, and interaction between neighbouring fish. Each particle represents a fish, or a group of fish.

The state variables of each particle are the position, time, speed and direction of movement, and the age and maturity level, although the last two variables are not considered in this paper. The main dynamic process is that the particles move with fixed time-steps, and the speed and direction of movement depend on the position of neighbouring particles and the surrounding temperature. In addition, the particles are moved by the oceanic current. The full model with environmental factors is described below.

The design concept is that a particle senses the positions of neighbouring particles as well as the temperature gradient, and adjusts its movement in terms of direction and speed for the next time-step according to these factors. There is no stochasticity in the present models, so the design parameters are as follows:

(i) time-step Δt;

(ii) radius of repulsion r_r, radius of alignment r_o, radius of attraction r_a, see Figure 1;

(iii) range of preferred temperature $[T_1, T_2]$, see Equation (5) later, and Figure 2;

(iv) relative weights of influence of neighbouring elements and temperature, β, see Equation (7).

Although not addressed here, the last two parameters could depend on maturity and age. As these biological variables are not active state variables in the present model, we include the influence of maturity by changing the speeds at a fixed longitude. We also note that when each particle represents a group of fish, as is the case here, the radii of interaction as well as the time-step have to be scaled.

The simulation is initialized by grouping the particles in patches at locations indicated by actual observations. The particles

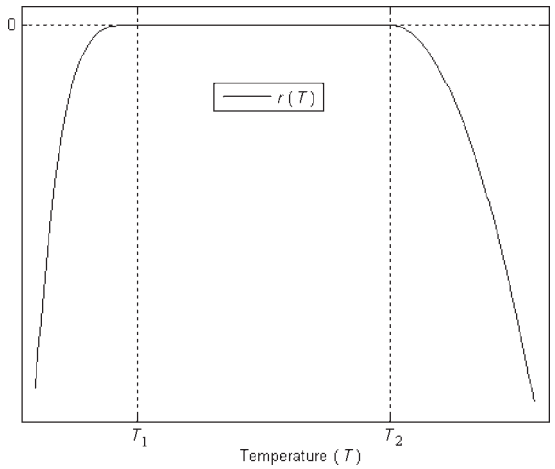

Figure 2. Graph of the temperature response function r from Equation (5).

are evenly distributed within the patch, but the initial direction of movement is random and the initial speed is set between 0 and 4.5 km d^{-1}. We give details of the parameter values and implementation below.

The input to the model is a map of oceanic currents and sea temperature. The map of oceanic currents did not vary with time in the simulations presented here, but demonstrates in a qualitative way the main features of the observed currents. We used one temperature map for each simulation because the simulated period is relatively short. These temperature maps were obtained by spatial interpolation of measured temperatures at selected locations.

The mathematical model

The model is a discrete off-lattice interacting particle model, and each particle represents an individual or a group of individuals. Particles look to their neighbours to determine their directional heading at each time-step, averaging the neighbours' directional headings to determine their own. This allows the particles to move together as a group. The model introduced in Vicsek *et al.* (1995), and further analysed and developed in Czirók *et al.* (1997, 1999) and Czirók and Vicsek (2000), is hereafter called

the CV model. This type of model originated in physics and was adapted by the biological community to model group dynamics of social animals. It has been applied to herds of mammals, swarms of locusts, and schools of fish (Vicsek *et al.*, 1995; Czirók *et al.*, 1997; Couzin *et al.*, 2002; Buhl *et al.*, 2006). A European project called STARFLAG (http://angel.elte.hu/starling) uses similar models for swarms of starlings and explores various interdisciplinary connections.

Experiments have shown that fish interact differently with each neighbour depending on the distance to the neighbour; fish use their vision and their lateral lines, sense organs running down the sides of many species, to align themselves with neighbours and organize themselves into schools (Partridge and Pitcher, 1980; Partridge, 1982). Fish tend to both aggregate and avoid collisions when travelling, and the number of and the distance to nearest neighbours seem to play a role in the organization of a school (Viscido *et al.*, 2004, 2005; Grünbaum *et al.*, 2005).

To simulate the internal dynamics of a group of interacting animals, many models incorporate different sensory regions into their simulations. The distance between two particles in such models determines how they react to each other and the strength of this interaction. These models include both individual and continuum (density) models, and the shape and the size of the sensory regions tend to differ depending on the model (see e.g. Couzin *et al.*, 2002; Kunz and Hemelrijk, 2003; Hemelrijk and Kunz, 2005; D'Orsogna *et al.*, 2006; Kunz *et al.*, 2006; Topaz *et al.*, 2006; Chuang *et al.*, 2007).

We follow Aoki (1982) and Huth and Wissel (1992) in employing three sensory zones around each particle to determine its reaction to the particles around it. Unlike many similar models, we do not employ a blind region behind the particle. It is ambiguous whether this blind region is biologically relevant for fish, because the lateral line could allow a fish to sense the region behind it as it swims. In addition, the presence of such a region does not seem to affect the outcome of simulations (Huth and Wissel, 1994).

Partridge (1982) pointed out that fish align their velocity to that of their neighbours. This feature was first introduced into the CV model by Hubbard *et al.*, (2004). Birnir (2007) analysed the continuous time limit of this type of model and found several solutions and symmetries. In Barbaro *et al.* (in press), solutions to both models presented in Birnir (2007) were verified numerically. With sensory zones added, the discrete model exhibits rich behaviour, and swarming solutions induced by noise were found. That work explored the interdependence of noise and the size and weights of the sensory zones in eliciting certain behaviour from the model.

We now describe the mathematical model in detail. The sensory zones are three regions around each particle, defined as shown in Figure 1. The innermost region is the zone of repulsion, and a particle heads directly away from other particles in this region, so avoiding collisions. The outermost region is the annular zone of attraction; a particle heads directly towards other particles in this region, adding to the cohesiveness of a group of particles. The annular region between the zones of repulsion and attraction is referred to as the zone of orientation, and a particle attempts to align itself in speed and in direction with particles within this zone. These directional headings often conflict, so each particle takes a weighted average of these directions, see Equations (3) and (4).

We denote the set of indices of the particles within particle k's zone of repulsion at time t by $R_k(t)$, its zone of orientation by $O_k(t)$, and its zone of attraction by $A_k(t)$. To simplify the notation, we omit the dependence on time below. At all times $k \in O_k$, ensuring that particle k's directional heading is taken into account. The number of particles within each zone is denoted by $|\cdot|$.

Let $\mathbf{q}_k(t) = (x_k(t), y_k(t))^{\mathrm{T}}$ and $v_k(t)$ denote the position and speed of particle k at time t, respectively. The particles then update their speeds as

$$v_k(t+\Delta t) = \frac{1}{|O_k|}\sum_{j\in O_k} v_j(t), \tag{1}$$

and their positions

$$\mathbf{q}_k(t+\Delta t) = \mathbf{q}_k(t) + \Delta t v_k(t+\Delta t)\begin{pmatrix}\cos(\phi_k(t+\Delta t))\\ \sin(\phi_k(t+\Delta t))\end{pmatrix}, \tag{2}$$

where $\phi_k(t)$ is the directional angle of particle k. To avoid conflicts with neighbouring particles, a weighted average is taken and $\phi_k(t+\Delta t)$ is calculated as

$$\begin{pmatrix}\cos(\phi_k(t+\Delta t))\\ \sin(\phi_k(t+\Delta t))\end{pmatrix} = \frac{\mathbf{d}_k(t+\Delta t)}{\parallel \mathbf{d}_k(t+\Delta t)\parallel}, \tag{3}$$

where

$$\mathbf{d}_k(t+\Delta t) := \frac{1}{|R_k|+|O_k|+|A_k|}\times\left(\sum_{r\in R_k}\frac{\mathbf{q}_k(t)-\mathbf{q}_r(t)}{\parallel \mathbf{q}_k(t)-\mathbf{q}_r(t)\parallel} + \sum_{o\in O_k}\begin{pmatrix}\cos(\phi_o(t))\\ \sin(\phi_o(t))\end{pmatrix} + \sum_{a\in A_k}\frac{\mathbf{q}_a(t)-\mathbf{q}_k(t)}{\parallel \mathbf{q}_a(t)-\mathbf{q}_k(t)\parallel}\right). \tag{4}$$

The environment

To model the migration route accurately, we include environmental data in the simulations to allow particles to respond to their environment. To this end, we introduce an environmental grid containing information about the current and the oceanic temperature at a depth of 50 m. The grid also has information about landmasses, encoded as points on the grid with extreme heat. The data contained in the grid allow each fish to be translated by the current and to adjust its direction depending on the temperature of the surrounding ocean.

The speed of a migrating capelin has been recorded at >25 km d^{-1} (Vilhjálmsson, 1994). The clockwise coastal current around Iceland is quite strong, and its speed can be of the same order of magnitude as the speed of fish relative to the surrounding sea. Although the current changes seasonally and even varies from day to day based on weather conditions, for simplicity we take it to be constant. Its maximum translation in the simulations is $\sim$15 km d^{-1} (Figure 3). We assume that fish do not change directional heading dependent on the current, so it translates them independent of their own movement. This assumption is reasonable and in fact integral to the physicality of the model, because in some years a portion of the capelin stock migrates anticlockwise around Iceland, against the current. We employ the same approximated oceanic current field as Magnússon *et al.*, (2005). Hereafter, the current field is denoted by **C**.

To model the capelin's reaction to the temperature of surrounding water, we extrapolate measured temperature data into

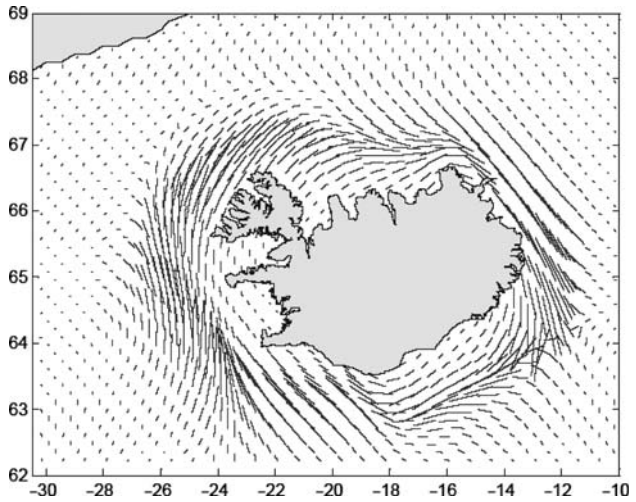

Figure 3. Simulated ocean current field around Iceland. The strength of the current is given by the length of the line segments. The stronger coastal current runs clockwise around Iceland.

a temperature field, denoted by $T(x, y)$. To create the temperature field for the simulations, we use available data from February of the years which we simulate. In the 1984–1985 and 1990–1991 case studies, presented in the Results section, we used temperature data recorded by the Marine Research Institute (MRI) of Iceland at a depth of 50 m at several locations in the sea around Iceland. The collection of data points for 1985 and 1991 is shown in Figure 4a and b. We extrapolated the temperature field from these data points, using Ocean Data View (Schlitzer, R., Ocean Data View, http://odv.awi.de, 2007).

In the 2007–2008 case study, we use temperature data extracted from a German weather website (http://www.wetterzentrale.de/topkarten/fsfaxsem.html) on 5 February 2008. These data were then extrapolated to our grid using Ocean Data View. The nature of these data is different from the data from the MRI, which had not been collected at that time; the website averages data from various surface measurements from buoys, satellites, and ships. If data are missing or beyond a certain distance from available measurements, the website uses the average temperature of the current month from 1961 to 1990. It is reasonable to assume that these surface data approximate the temperature at a depth of 50 m because, in winter, strong winds and storms cause turbulent mixing of the water near the surface down to a few dozen metres, as temperature data corroborate. Hence, the temperature data are comparable among these three case studies. Contour plots of the extrapolated temperatures are shown in Figure 4.

The particles sense the surrounding temperature, T, according to the gradient of the function r (Figure 2):

$$r(T) := \begin{cases} -(T - T_1)^4 & \text{if} \quad T \le T_1 \\ 0 & \text{if} \quad T_1 \le T \le T_2 \\ -(T - T_2)^2 & \text{if} \quad T_2 \le T, \end{cases} \tag{5}$$

where T_1, T_2 are constants, and $[T_1, T_2]$ is referred to as the preferred temperature range. By looking at the gradient of r, we see that fish should move towards areas within the preferred temperature range, the tendency being stronger in colder water.

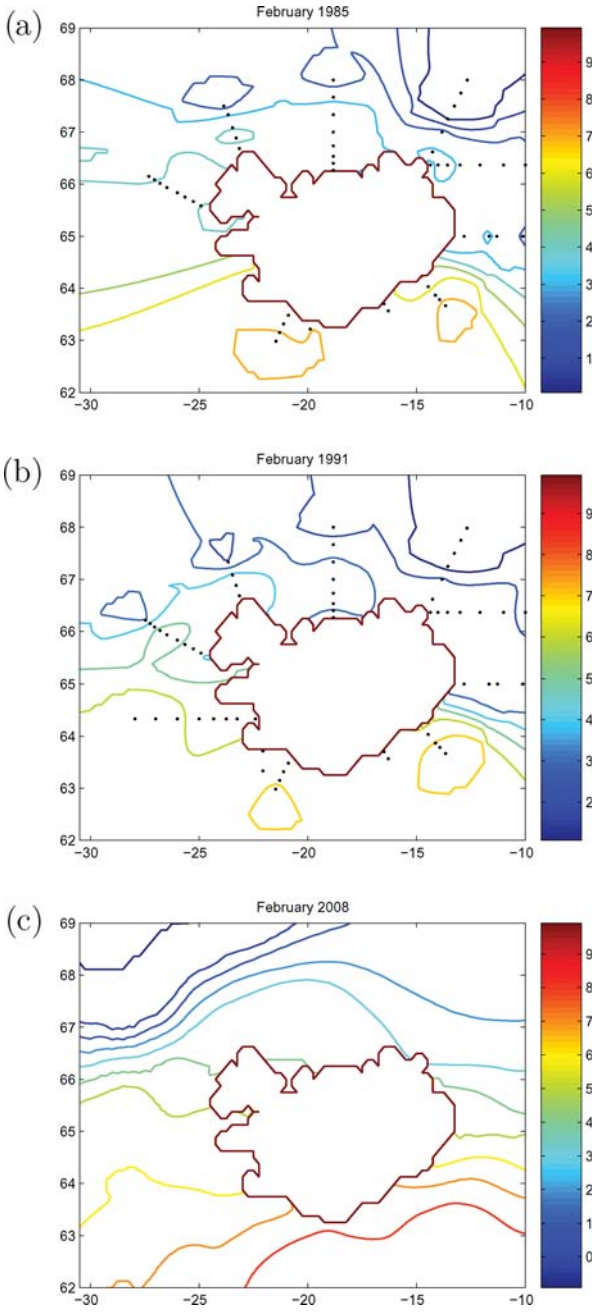

Figure 4. Contour lines of extrapolated temperature data used in the simulations. The black dots in (a) and (b) show locations of measurement points. From February of (a) 1985, 50 m depth, (b) 1991, 50 m depth, and (c) 2008, surface temperature.

Including the environmental fields, Equation (2) becomes

$$\mathbf{q}_k(t + \Delta t) = \mathbf{q}_k(t) + \Delta t v_k(t + \Delta t) \frac{\mathbf{D}_k(t + \Delta t)}{\| \mathbf{D}_k(t + \Delta t) \|} + \mathbf{C}(\mathbf{q}_k(t)), \tag{6}$$

where

$$\mathbf{D}_k(t + \Delta t) := (1 - \beta) \frac{\mathbf{d}_k(t + \Delta t)}{\| \mathbf{d}_k(t + \Delta t) \|} + \beta \frac{\nabla r\big(T(\mathbf{q}_k(t))\big)}{\| \nabla r\big(T(\mathbf{q}_k(t))\big) \|}. \tag{7}$$

We let $\beta \in [0, 1]$. The speed v_k is calculated as in Equation (1), $\mathbf{C}(x, y)$ is the current, and $\mathbf{d}_k$ the same unit vector as in Equation (4). The factor β, to which we refer as the temperature weight factor, determines the relative weight of each particle's reaction to the temperature field compared with the interaction with its neighbours. The model's behaviour is highly dependent on this parameter, as discussed below.

Parameter and simulation specifications

In the simulations, we use a general *xy*-coordinate system of dimensions 82 by 56. The temperature and oceanic currents are stored in a grid defined at points $(i, j) \in \mathbb{Z}^2 \cap ([0, 82] \times [0, 56])$, corresponding to the area from 30.5–10.0°W to 62.0–69.0°N. Hence, the spacing between points on the environmental grid is 0.25° in longitude and 0.125° in latitude. This means that the grid has a spatial resolution of roughly 12 km in each direction, although the longitudinal length varies slightly depending on the latitude. This discrepancy is not significant for our simulations, so is not taken into account here.

We initially placed particles in areas where data indicated a high density of mature capelin (Vilhjálmsson, 1994). We held the number of particles per "main school" to be between 40 000 and 50 000 in each simulation, with a uniform density in each school across the simulations. This ensures that the dynamics of the migration are similar across years, although the total number of particles differs between simulations. According to the scaling laws presented below, by keeping the particle density constant in areas containing fish, we avoid the need to change parameter values between simulations.

Icelandic capelin generally spawn in water between 3 and 10°C (Vilhjálmsson, 1994). In the simulations, we set the temperature preferences to be between 3 and 6.5°C. Interaction among particles paired with a high interaction weight enables particles to enter water that is outside their preferred range. We set the temperature weight factor $\beta = 0.01$ [Equation (7)], but because of the form of the temperature preference function (5), the particles tend to leave water that is drastically different from their preferred range. This preference function combined with the fact that all the particles are reacting to the same temperature map keeps them in water of a temperature close to the actual preferred range of the capelin.

We measure time t in days and speed v_k in grid units ($\sim$12 km) per day, and the radii of a particle's sensory zones in grid units. We set $\Delta t = 0.05$ (i.e. 1.2 h); speeds v_k were initialized uniformly in [0, 0.375] (i.e. [0, 4.5] km d^{-1}), then updated according to Equation (1). Initial direction angles are assigned randomly. Once the particles are east of 13.5°W, the algorithm sets $v_k = 1.25$, or $\sim$15 km d^{-1}, which is significantly faster than the initial speeds and crudely models the observed increase in speed.

With our choice of Δt and v_k, each particle travels on average 0.12 km per time-step. This means that it takes a particle about 100 time-steps to move from one grid point to another. As described in the next section, refining the temporal resolution will result in a refined spatial resolution. Taking time-steps that are too large for the grid resolution would force particles to skip over grid points, and therefore to miss the information located at these grid points. By choosing Δt and v_k as we have, we are simulating at the resolution of the environmental data, thereby using all the information available. This indicates that refining the time-step will not change the behaviour and dynamics with respect to the environmental fields.

The other parameter values were $r_r = 0.010$ and $r_o = 0.100$, which correspond roughly to $r_r \simeq 120$ m and $r_o \simeq 1.2$ km. We found that including the zone of attraction causes the particles to cluster unnaturally and fails to reproduce the large schools observed by researchers. The zone of attraction was therefore excluded here from the simulations by setting $r_a = r_o$.

In the simulations of the three spawning migrations, which are presented in the Results section, the parameter values are therefore

$$\begin{aligned} \Delta t &= 0.050, \\ (r_r, r_o, r_a) &= (0.010, 0.100, 0.100), \\ [T_1; T_2] &= [3.0; 6.5]^\circ\mathrm{C}, \\ \beta &= 0.010. \end{aligned} \tag{8}$$

We note that with these parameter values, the spatial resolution Δq is similar to the radius of repulsion, r_r. When a particle updates its directional heading, it takes into account all neighbouring particles that it could encounter in the next time-step. This ensures that particles tend to avoid collisions at each time-step.

Finally, the code used is written in C++, and the run time with around 50 000 particles was on average 3–5 h. All simulations were done on a dual-core Intel Pentium 4 (2.60 GHz per core, 512 L2 cache, 1 GB main memory). For further details about the implementation, and how the simulations can be run in parallel, see Youseff *et al.* (2008).

Scaling

When working with discrete interacting particle models, it must be emphasized how parameters scale in relation to each other. When a particle represents many individuals, we think of the particle as a school of fish all behaving in an identical manner to a single individual. We call these particles superindividuals. We are assuming that the dynamics of a school of superindividuals is identical to those of a large school of individuals, which we justify with the scaling arguments presented below. Note that finding the correct interactions among superindividuals is a different problem that is not addressed here.

For a given year, let F be the number of individual fish in the actual migration. For the sake of simplicity, we take F to be constant, despite predation and other natural factors. Also, let N be the number of particles in a given simulation. Define $F^s := F/N$ to be the number of fish that each particle, or superindividual, represents in that simulation.

We let Δq denote the distance a particle travels in one time-step at speed v. The simple relationship $\Delta q = v\Delta t$ indicates that there is a linear scaling between the spatial and the temporal variables:

$$\Delta q \propto \Delta t. \tag{9}$$

Here, the time-step Δt is a parameter in the simulations and we use Δq as a measure of the spatial resolution in the simulations.

The radii of the zones of repulsion r_r, orientation r_o, and attraction r_a are parameters which are known in the literature to affect the behaviour of the system (Huth and Wissel, 1992; Couzin *et al.*, 2002; D'Orsogna *et al.*, 2006). We assume that $r_r \propto r_o \propto r_a$.

Each particle travels a distance of Δq at every time-step and senses other particles within its sensory zones. In order for the movements and interactions among particles to be consistent across simulations, the radii of these sensory zones should also

scale with Δq, i.e.

$$\Delta q \propto r_\gamma, \qquad \gamma \in \{r, o, a\}, \tag{10}$$

and from Equation (9) we see that the same holds for Δq replaced by Δt.

When adding more particles to the system, we require the dynamics of the simulations to be comparable. Let us consider the number of fish in a region of area R, assuming uniform density. Let us now spread N superindividuals evenly throughout this region. Then each superindividual in effect represents the fish contained in an area of R/N. Thus, as the number of superindividuals increases, the number of fish which each particle represents decreases with this area. We assume that $(\Delta q)^2$ scales with the size of the area of the region which each superindividual represents. Therefore,

$$\Delta q \propto \frac{1}{\sqrt{N}}, \tag{11}$$

or equivalently

$$\Delta q \propto \sqrt{F^s}, \tag{12}$$

because $F^s := F/N$. First, this ensures that the number of particles that each particle will interact with during one time-step will not depend significantly on F^s. Second, from Equation (10), the same holds for the number of particles within each zone of interaction.

One ambitious goal of our research is to be able to simulate each fish in the migration. In Youseff *et al.* (2008), the run time of the code is shown to be $O(N^{1.8})$, when run in parallel. Using relations (9) through (11), it is of interest to investigate how the parameters should scale when we take $F^s = 1$, i.e. when each particle in the simulation corresponds to one fish. In the simulation which accurately reproduces the spawning migration of 2008, the number of particles is in the order of 5×10^4. A conservative estimate of the stock size of the migrating capelin is $F \simeq 5 \times 10^{10}$ individual fish. Thus, the number of fish each superindividual represents in our case studies is $F^s \simeq 10^6$.

When simulating individuals, i.e. when $N = F$, the spatial resolution can be calculated to be $\Delta q \simeq 12$ cm and the temporal resolution to be $\Delta t \simeq 4.3$ s. The radius of repulsion should scale down to $r_r \simeq 12$ cm, which is just under 1 body length. The radius of orientation should scale to $r_o \simeq 1.2$ m. It is worth noting that these values are quite reasonable from a biological perspective (Partridge and Pitcher, 1980; Partridge, 1982). Furthermore, modern computational capabilities should allow for simulations at this scale, allowing us to model at the level of an individual.

Results

The scenarios and sensitivity analysis presented below identify two parameters key to recreating the migration route from a given year: β, the relative weight a particle places on the temperature term to determine its next directional heading, and $[T_1, T_2]$, the particles' preferred temperature range. The system is sensitive to perturbations in either of these two parameters. Using parameter values described in Equation (8), we closely replicate the spawning migration route of the Icelandic capelin from three different years. In particular, the simulations recreate characteristics of the migration route particular to each of the 3 years we consider, closely matching acoustic data (Vilhjálmsson, 1994).

Three spawning migrations

The first simulated migration was the spawning migration during winter of 1984–1985. We ran the simulation for 2200 time-steps, or 110 d, starting in mid-November. Figures 5–7 show acoustic data from Vilhjálmsson (1994) juxtaposed with simulation pictures corresponding to approximately the same period. In Figure 5, we show the acoustic data gathered between 1 and 21 November 1984 alongside the simulation's initial distribution of particles.

Figure 6a shows acoustic measurements taken between 14 January and 8 February 1985, and Figure 6b shows day 65 of the simulation, corresponding to mid-January 1985. In both pictures, the main school is travelling along the east coast of Iceland. Note that the simulation accurately captures the high density within the school farthest to the south, as can be seen by the red shading of this section of the school. The difference between the acoustic data and the simulation to the northwest can be explained by emergence of fish from beneath the ice sheet. The model does not add particles during simulations, so does not replicate the dynamics of the emerging fish.

Figure 7a shows the acoustic data from 7 to 20 February 1985 at a different location from that shown in Figure 6a, and Figure 7b shows day 109 of the simulation, corresponding roughly to late February. Both pictures show a school coming close to shore on the east coast of Iceland. Note here that the simulation shows an

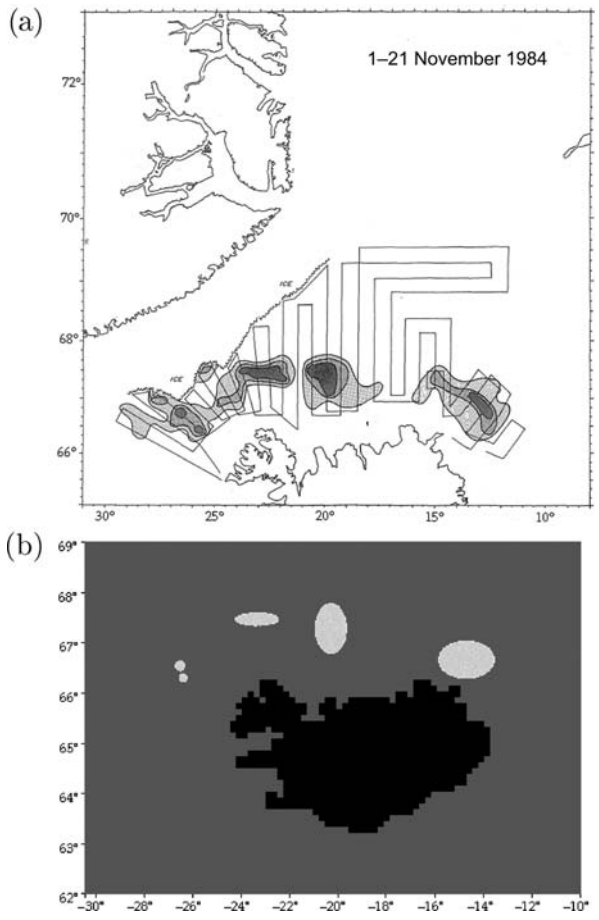

Figure 5. The distribution of capelin in November 1984. (a) Acoustic data from 1 to 21 November (after Vilhjálmsson, 1994). (b) Initial distribution for the simulation.

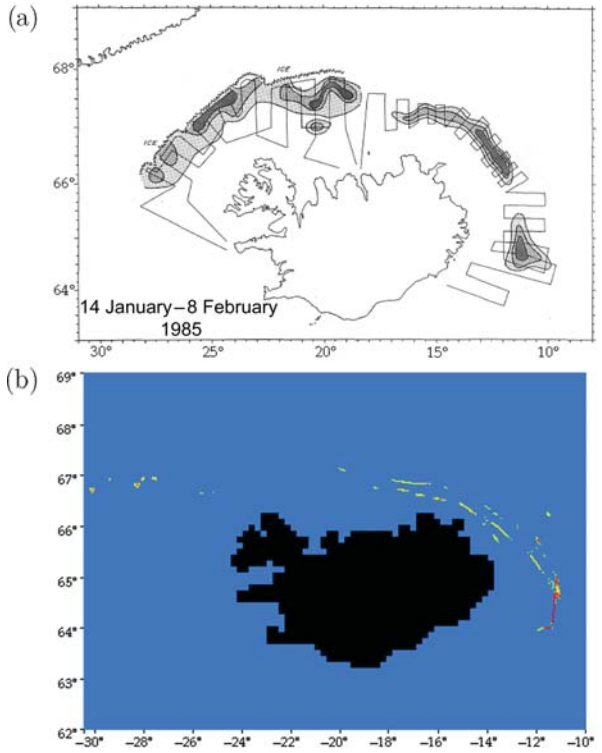

Figure 6. The distribution of capelin from mid-January to early February of 1985. (a) Acoustic data from 14 January to 8 February (after Vilhjálmsson, 1994). (b) Simulated distribution in mid-January, day 65 of the simulation.

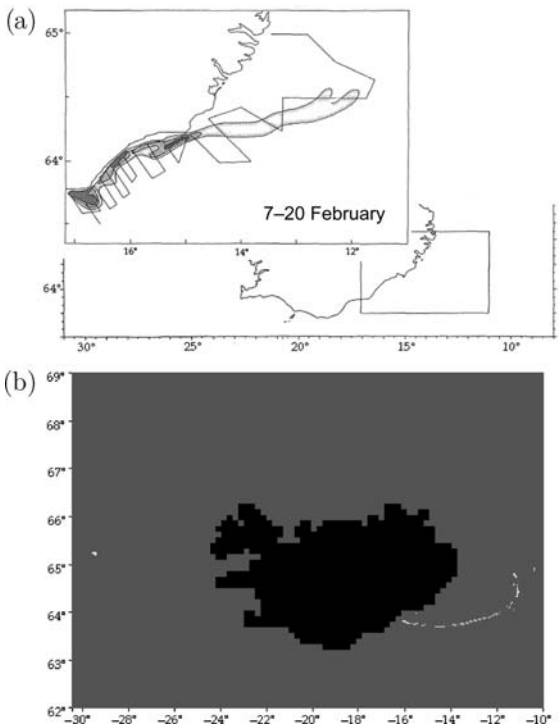

Figure 7. (a) Close up of the distribution of capelin from 7 to 20 February 1985 (after Vilhjálmsson, 1994). (b) Simulated distribution in late February, day 109.

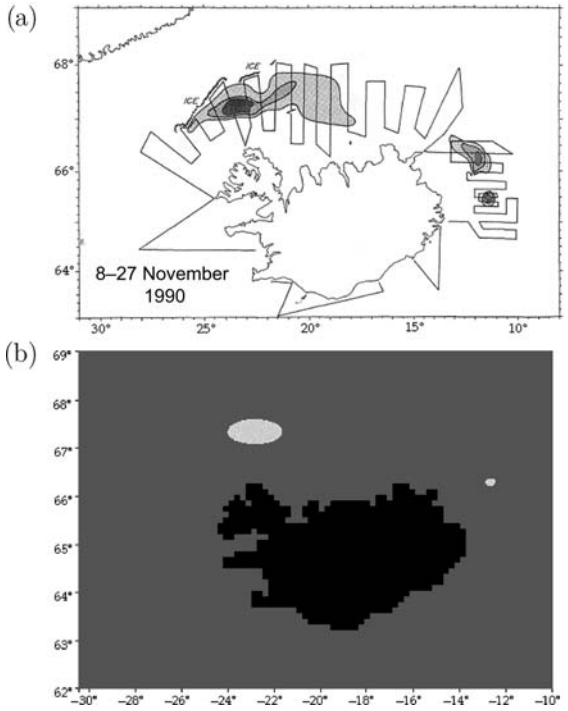

Figure 8. The distribution of capelin in November 1990. (a) Acoustic data from 8 to 27 November (after Vilhjálmsson, 1994). (b) Initial distribution for the simulation.

elongated school of particles heading into shore at a similar latitude to that indicated by the acoustic data, although the particles are not as close to the shore in the simulation.

With parameter values identical to the 1984–1985 simulation, we model the 1990–1991 spawning migration. We run this simulation for 1900 time-steps, or 95 d. In this case, the particles are placed where data indicate that the capelin were between 8 and 27 November 1990 (Vilhjálmsson, 1994). In Figure 8, we show these acoustic data next to the initial placement of particles for this simulation. Figure 9a shows the acoustic data gathered between 4 and 11 January 1991, and Figure 9b the simulation of day 44, corresponding to early January. Both Figure 9a and b show a cohesive school travelling clockwise to the east of Iceland. The location of the front of the school is similar between the two, although in the simulation, the tail of the school was closer to Iceland than indicated by the acoustic measurements. The lines in Figure 9a show where research vessels searched for capelin; we cannot assess the accuracy for the schools located outside this area in the simulation.

In Figure 10, acoustic measurements from 8 to 9 February 1991 are shown alongside day 66 of the simulation, corresponding to early February. The simulation indicated that a school of particles headed to the shore, as the acoustic data show. However, the particles in the simulation were farther south and west than in the acoustic measurements. In Figure 10b, there is also a large number of particles in the southeast corner of the simulation not corroborated by the measurements. This atypical route could be caused by the extrapolation used to make the temperature data for the simulations, but see the Discussion section for further detail. Figure 11 juxtaposes acoustic data gathered on 17 and 18 February 1991 with the simulation in mid-February, on day 72. Note that the simulation shows two schools of particles near the

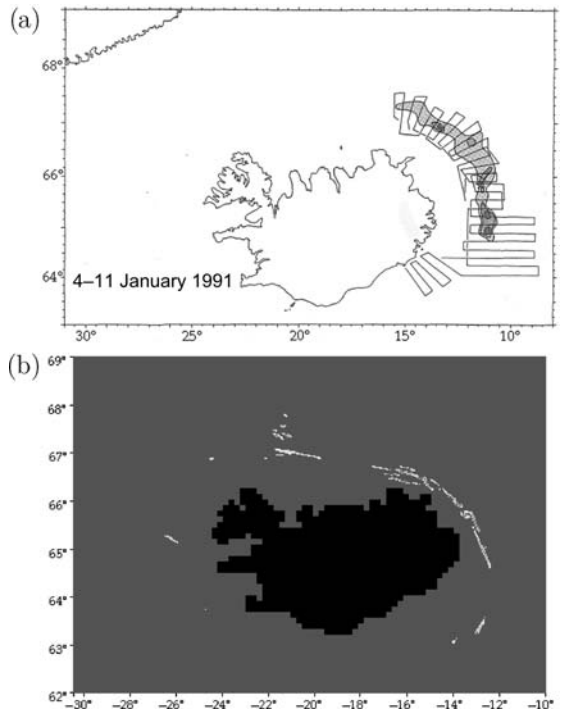

Figure 9. The distribution of capelin in January 1991. (a) Acoustic data from 4 to 11 January (after Vilhjálmsson, 1994). (b) Simulated distribution in early January, day 44 of the simulation.

southwestern shore of Iceland, precisely where the acoustic measurements indicated the highest density to be. This is a notable difference from the route of the 1984–1985 migration.

A very important result is the successful prediction of the route of the 2007–2008 spawning migration using only initial fish density and temperature measurements taken by research and fishing vessels during January 2008. Capelin proved to be difficult to find, and a very low fishing quota was set. Subsequently, the fisheries were closed in late February as a result of poor and low estimates of stock size. Eventually, a large quantity of capelin was found to have taken an unusual route, resulting in an additional fishing quota being set at the beginning of March 2008.

We run the 2007–2008 simulation for 1900 time-steps (95 d) between early January and early April. Figure 12 shows the simulated migration's initial placement and simulations of days 47, 59, and 65, roughly mid-February, late February, and early March. Figure 13a shows acoustic measurements from 26 to 27 February, and Figure 13b shows observations gathered between 29 February and 3 March. Comparing Figure 12c with Figure 13a reveals that the bulk of the particles in the simulation headed towards the shore almost exactly where the research vessels later found them to be. Furthermore, Figure 12d shows a school of particles east of Iceland in almost precisely the same location as the school of fish farthest to the right in Figure 13b. This indicates that the route and proportions of the particles in the simulated spawning migration were remarkably accurate, especially because the simulation was completed in early February 2008, before fishing was closed.

Sensitivity analysis

We now look more closely at the behaviour of the model when parameters are varied. We choose the run from the 2007–2008

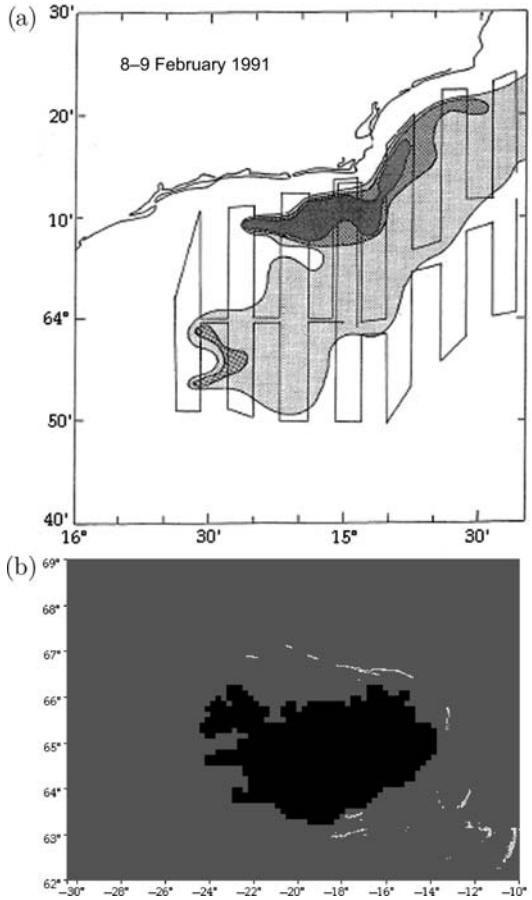

Figure 10. (a) Close-up of the distribution of capelin southeast of Iceland from 8 to 9 February 1991 (after Vilhjálmsson, 1994). (b) Simulated distribution in early February, day 66.

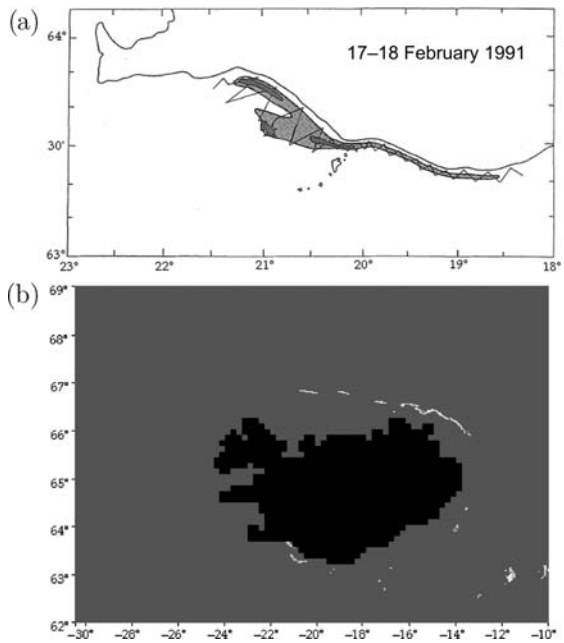

Figure 11. The distribution of capelin southwest of Iceland in February 1991. (a) Acoustic data from 17 to 18 February (after Vilhjálmsson, 1994). (b) Simulated distribution in mid-February, day 72.

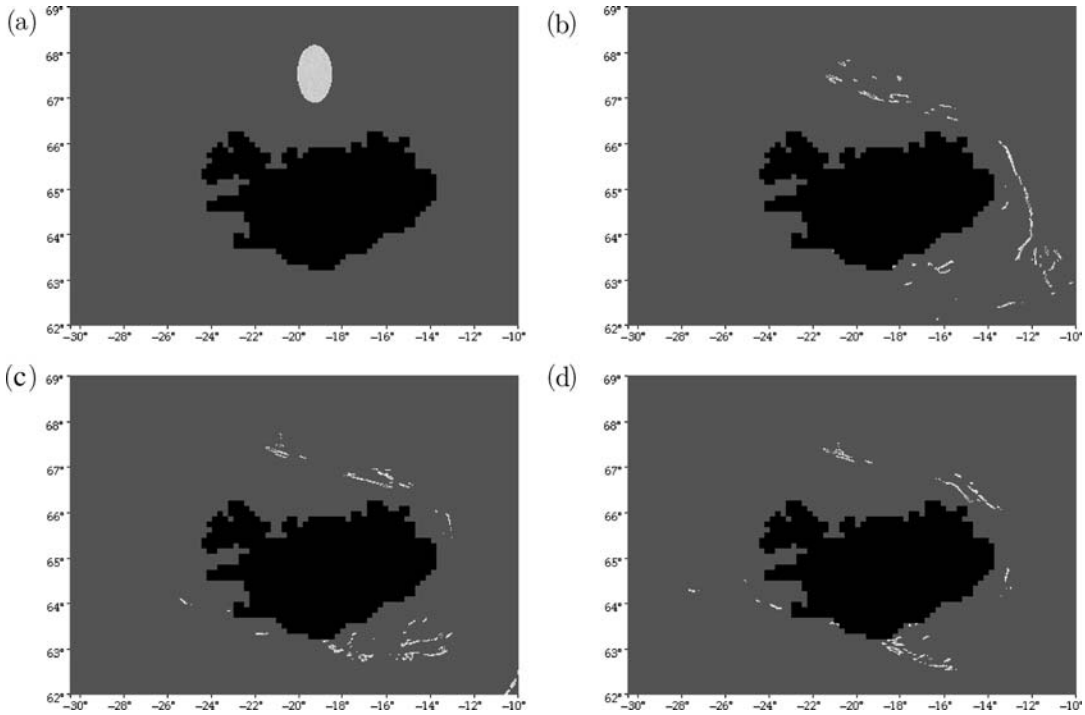

Figure 12. Simulation of the 2007–2008 spawning migration. (a) Early January, day 0, (b) mid-February, day 47, (c) late February, day 59, and (d) early March, day 65.

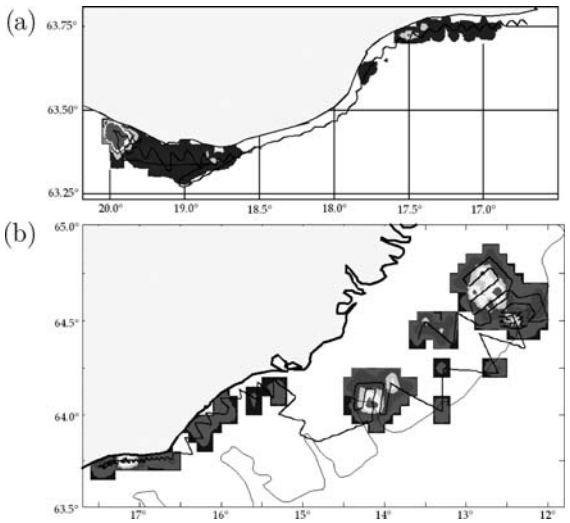

Figure 13. (a) Measured distribution of capelin near the south coast of Iceland from 26 to 27 February 2008. (b) Measured distribution of capelin near the southeast coast of Iceland from 29 February to 3 March 2008.

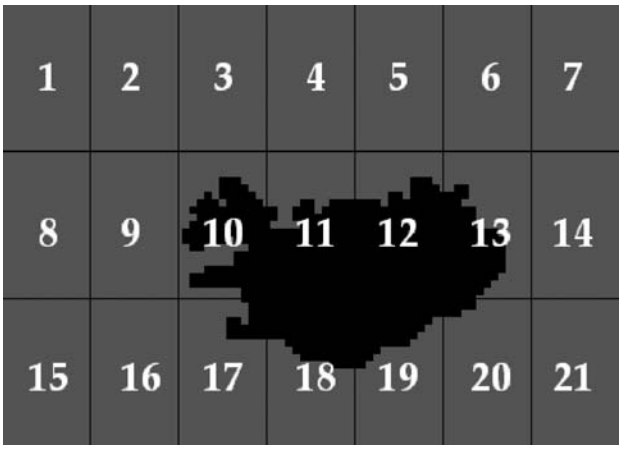

Figure 14. Compartments used for the sensitivity analysis. See section on the sensitivity analysis and Tables 1–3.

simulation as a reference case with which we compare the other simulations. This choice of parameters successfully predicted the unusual spawning migration of that year, in addition to producing good results for the two other years.

To quantify the outcome of the sensitivity analysis, the area of the simulation is divided into 21 numbered compartments, as shown in Figure 14. In each new simulation, only one parameter value is changed to understand its role in the model. The new values for each parameter are presented in Table 1, giving rise to nine scenarios.

The number of particles in all runs was ~41 800. At days 47 and 65, the numbers of particles in each compartment were counted, then divided by the initial number of particles in these simulations to obtain the distribution as percentages. This was done for Scenarios (a)–(i) (Table 1) as well as the 2007/2008 reference case on days 47 and 65 (Tables 2 and 3). Note that the percentage values of the reference simulation do not add up to 100% nor do the differences in the remaining simulations add up to 0%. The reason is that particles crossing the boundary of the model region

Table 1. Parameter values used in scenarios of sensitivity analysis.

Parameters varied	Lost on day 47 (%)	Lost on day 65 (%)
(a) $T_2 = 7.5^\circ$C	10.7	14.7
(b) $T_1 = 2.0^\circ$C	18.4	22.7
(c) $\beta = 0.002$	38.3	64.9
(d) $\beta = 0.005$	9.3	23.4
(e) $\beta = 0.015$	9.0	11.1
(f) $\beta = 0.050$	12.3	72.4
(g) $r_r = 0.005$	14.5	29.8
(h) $r_r = 0.020$	4.6	7.6
(i) $r_a = 0.200$	8.8	10.0

Parameter values used in the reference case of 2007–2008: $[T_1; T_2] = [3.0; 6.5]^\circ$C, $\beta = 0.010$, $(r_r, r_o, r_a) = (0.010,0.100,0.100)$.

Table 2. The entries in the first block show the distribution into the compartments shown in Figure 14 on day 47 in the reference case of the 2007–2008 simulation, which is described in the Results section.

Day 47	0.0	0.0	0.0	13.2	3.2	0.0	0.0
	0.0	0.0	0.0	0.0	1.2	22.0	13.0
	0.0	0.0	0.0	0.6	7.4	8.0	22.5
(a)	0.0	0.0	1.9	0.6	1.2	0.0	0.0
	0.0	0.0	0.0	0.0	4.6	14.9	−9.2
	0.0	0.0	0.0	0.7	−1.8	1.7	−16.5
(b)	0.0	0.0	6.4	−1.5	14.3	19.3	0.3
	0.0	0.0	0.0	0.0	−1.2	−9.2	−12.2
	0.0	0.0	0.0	3.8	−2.4	−4.8	−22.5
(c)	0.0	0.0	4.6	−4.8	−0.1	8.3	0.0
	0.0	0.0	0.0	0.0	−1.2	−11.0	−3.5
	0.0	0.0	0.0	−0.6	−7.2	0.1	−14.1
(d)	0.0	0.0	0.0	9.5	7.2	2.5	0.0
	0.0	0.0	0.0	0.0	−1.2	3.1	−11.1
	0.0	0.0	0.0	1.5	4.4	−6.9	−9.5
(e)	0.0	0.0	0.0	−8.6	3.1	1.2	0.0
	0.0	0.0	0.0	0.0	3.1	4.8	−10.4
	0.0	0.0	0.0	−0.6	−0.1	15.3	−8.0
(f)	0.0	0.0	0.0	−6.1	3.9	0.3	0.0
	0.0	0.0	0.0	0.0	−1.2	−10.2	37.5
	0.0	0.0	0.0	−0.6	−7.4	−2.7	−17.1
(g)	0.0	0.0	0.0	−1.3	−2.7	0.0	0.0
	0.0	0.0	0.0	0.0	1.0	−2.1	−5.3
	0.0	0.0	0.0	3.1	−1.5	6.1	−3.1
(h)	0.0	0.0	0.0	−11.2	−2.9	0.0	0.0
	0.0	0.0	0.0	0.0	2.5	−0.3	−10.5
	0.0	0.0	0.0	2.9	6.4	8.6	8.8
(i)	0.0	0.0	0.0	−6.1	6.5	0.1	0.0
	0.0	0.0	0.0	0.0	−1.2	7.9	−3.2
	0.0	0.0	0.0	−0.1	2.9	15.7	−22.5

For a description of Scenarios (a)–(i) see Table 1, and the difference between the scenarios and the reference simulation of 2007–2008 is shown. The entries in (a)–(i) correspond to the compartments shown in Figure 14, and a negative entry signifies more particles being in the reference simulation of 2007–2008.

Table 3. The entries in the first block show the distribution into the compartments shown in Figure 14 on day 65 in the reference case of the 2007–2008 simulation, which is described in the Results section.

Day 65	0.0	0.0	0.0	7.3	6.0	0.0	0.0
	0.0	0.5	0.0	0.0	0.0	18.9	0.0
	0.0	0.4	11.1	19.6	7.6	1.7	6.7
(a)	0.0	0.0	2.6	−0.1	−0.9	0.0	0.0
	0.0	−0.5	0.0	0.0	0.0	9.1	0.0
	0.0	−0.4	3.1	−2.8	−0.1	2.3	−6.7
(b)	0.0	0.0	2.8	6.1	−4.7	0.5	0.0
	0.0	4.0	0.0	0.0	0.9	1.0	25.9
	0.0	−0.4	−3.4	−19.6	−7.1	−1.7	−6.7
(c)	0.0	0.7	3.8	−1.7	−5.4	4.3	0.0
	0.0	−0.5	0.0	0.0	0.0	−3.5	4.4
	0.0	−0.4	−10.9	−19.5	−7.6	−1.7	−6.7
(d)	0.0	0.0	0.2	2.6	3.7	0.4	0.0
	0.0	6.4	0.0	0.0	5.5	2.5	3.7
	0.0	3.6	−7.0	−18.6	−7.5	0.8	0.5
(e)	0.0	0.0	0.0	−7.3	−3.6	0.0	0.0
	0.0	−0.5	0.0	0.0	1.5	13.3	0.2
	0.0	−0.4	−11.1	−19.6	39.8	3.3	−6.4
(f)	0.0	0.0	4.8	−6.0	−5.3	0.0	0.0
	0.0	−0.5	0.0	0.0	0.1	−5.6	2.4
	0.0	−0.4	−11.1	−19.6	−7.6	−1.4	−2.0
(g)	0.0	0.0	0.0	−1.8	−1.8	0.3	0.0
	0.0	−0.5	0.0	0.0	0.0	−0.3	0.0
	0.0	3.8	6.9	−7.2	−0.5	−1.6	−6.7
(h)	0.0	0.0	0.2	−5.6	−5.6	0.0	0.0
	0.0	5.3	0.0	0.0	0.0	0.7	0.0
	0.0	−0.4	3.0	19.0	2.0	0.6	−6.6
(i)	0.0	0.0	0.0	−0.2	−6.0	0.0	0.0
	0.0	0.2	0.0	0.0	0.0	−5.9	0.0
	0.0	−0.4	6.1	−10.3	22.6	11.0	−6.6

The Scenarios (a)–(i) are described in Table 1, and the difference between the scenarios and the reference simulation of 2007–2008 is shown. The entries in (a)–(i) correspond to the compartments shown in Figure 14, and a negative entry signifies more particles being in the reference simulation of 2007–2008.

are lost. The percentage of lost particles in the reference case on days 47 and 64 was 8.9 and 20.3%, respectively.

In Scenario (a), only the upper bound of the preferred temperature range was increased. The runs therefore look similar until the particles reached the upper limit of the preferred temperature range in the east of Iceland. On day 47, the difference in compartments 13, 14, and 21 was the result of the particles not reaching this upper limit. They therefore stayed closer to shore and were in turn translated by the current to the south. The distribution on day 65 was, however, similar to the reference case. In Scenario (b), the lower bound of the temperature range was lowered and the particles lingered in the north (see compartments 5 and 6 on day 47). The reason for this is that the cold front in the north did not push the particles down into the stronger currents. The current then slowly moved the particles to the east, and on day 65 most of the particles were located in compartment 14. We note that the particles did not reach the spawning grounds, as compartments 17–19 showed.

In Scenarios (c)–(f), the value of β was changed. This parameter determines how strongly the particles sense their temperature environment compared with the strength of interaction. In Scenarios (c) and (d), the value of β was lowered, so the effect of the current was the main environmental factor in the particles' movement. They therefore did not sense the temperature as strongly, causing them to swarm to the north.

In extreme Scenario (c), where the value of β was one-fifth of the reference value, the particles travelled slowly to the northern and the eastern boundary, and close to 65% of the particles were lost. In Scenario (d), lack of an aggregate direction caused a more northerly distribution than in the reference case, on days 47 and 65. For both (c) and (d), the particles did not arrive at

the spawning grounds. In (c), a small proportion of the particles travelled south, but did not come close to land because the effect of temperature was not strong enough to drive them to shore. The particles passed by the spawning grounds and finished in compartments 9 and 16, far off the coast of Iceland.

Scenarios (e) and (f) had a higher value of β than in the reference simulation, so the particles sensed their environment more strongly. Interestingly, even in (e) with β 50% higher than in the reference case, the particles did not arrive at the spawning grounds. When they reached the 6.5°C isotherm, they were diverted to the west. Most of the particles then came to shore in southeast Iceland, because they were not able to enter water that was too warm. Close to 58% of the particles finished in compartments 12, 13, 19, and 20.

In Scenario (f), the high value of β resulted in an interesting behaviour when the particles reached the 6.5°C isotherm. The strong current translated the particles into warm water, to which they reacted strongly. Unable to enter the warm water, the particles were reflected to the east and continued off the boundary. About 72% of the particles were lost to the east in this way.

Finally, Scenarios (g)–(i) explored the behaviour of the system as the ratio of the radii changed. In Scenario (g), the radius of repulsion, r_r, was half the value used in the reference case, and in (h) it was twice the value. In Scenario (g), the particles formed smaller schools, because the small value of the radius of repulsion did not force them to spread out. Some particles reached the spawning grounds via a similar route to the reference case, but more quickly (see compartments 16–18 in Table 3). In Scenario (h), the particles also reached the spawning grounds similarly to the reference case. The main difference in distribution can be explained by the fact that many fewer particles were lost: in the reference case $>20\%$ were lost on day 65, but $<8\%$ in Scenario (h). The schools were also more spread out, as expected from a larger value of the radius of repulsion. Finally, Scenario (i) includes a non-trivial zone of attraction. In this case the particles clumped unnaturally and moved in small clusters. This led to less cohesion among the particles as a whole, which is uncharacteristic of the system (Vilhjálmsson, 1994).

Discussion

Our work indicates that it is possible to explain the migration route of the Icelandic capelin stock without a homing instinct, and that oceanic temperature is of great importance to the path of the migration. With tens of thousands of particles, information about the environment propagates through the simulated schools much more effectively than in previous models, which makes the system more able to sense the environment. This improvement could account for not needing attraction potentials to reproduce the migration.

The success of such a biologically simplistic model demonstrates the profound effects that temperature and local interaction among the fish have on the migration route. Using a preferred temperature range and an adjustable strength of the interactions between particles suffices to reproduce the spawning migration qualitatively. Although it is impossible to determine with certainty how organisms behave, one hopes to produce a model that is at least able to reproduce the behaviour. Doing so with a model that uses interaction strength and measured environmental factors is therefore a significant result for the model being used. The results also highlight the effect global warming can have on the ecology of the ocean.

The sensitivity analysis indicates that the value of β controls a fine balance between how strongly the particles sense their environment and the strength of interaction among particles. The value of β has to be high enough to allow a school to sense the environment, but low enough to allow it to enter water outside the preferred temperature range of the fish. It must be emphasized that the value of β seems to affect where the particles come onto the continental shelf of Iceland. This is an interplay between the currents and the shape of the temperature contour lines around Iceland (Figures 3 and 4). The fast current off the southeast coast drives the particles into warm water, and in return the value of β determines how the particles respond to that warm water.

We found that artefacts of the temperature extrapolation greatly affected the simulations in the 1990–1991 case study. The particles left the area for which we had accurate temperature readings, and entered the southeastern part of the grid where accurate data were not available. Owing to the effects of the temperature extrapolation in this region, the particles were likely to travel off the bottom of the grid. In the 1984–1985 simulation, the particles stayed generally within the area for which we had reliable temperature values based on interpolation rather than extrapolation. For the 2007–2008 simulation, we used data from the German weather map, so we had a more complete temperature map of the entire region than for the other years. Because of this, the particles in the simulation were reacting to actual temperature data regardless of their placement within the grid.

A point of interest is the difference between the weight factor β and the radii of interaction, r_r, r_o, r_a. As the radii depend on the number of particles (see the section on scaling), one might conclude that the weight factor should do the same. However, the weight factor governs the balance between the environmental data and the interactions for each particle. Therefore, it determines a behaviour which is indeed independent of the number of particles in the simulation, given that the number of neighbours within a particle's zone of interaction remains constant, as we assumed in the scaling arguments.

We note that the schools of particles in the simulations seem "thin" compared with acoustic measurements. Adding noise to the directional angle of the particles could have the effect of spreading them out. Noise has not been added into the simulations at this stage, to facilitate the interpretation of the behaviour of the system. Future simulations will incorporate noise, which requires a statistical interpretation of the simulations.

The fact that some groups of particles in the simulations tended to take different routes than expected from existing data indicates that additional factors affect the migration route. Good temperature measurements were available, but a more accurate and dynamic current field is needed. The most obvious information which needs to be included in simulating the spawning migration is the sexual maturity of the fish. The fish have been observed to wait on the boundary between warm and cold water until the mass of the roe content in the females reaches 8–10% of their body weight. Once they enter the warmer water, their maturation accelerates, which seems to drive them to seek out desirable conditions for spawning (Vilhjálmsson, 1994). In fact, the capelin is a benthic spawner, and depth and the substratum upon which it spawns play a role in the location of spawning. One possible extension to the model would be to add information regarding the substratum and the depth to the model in a similar way as temperature. The model currently uses no maturity cues, so

cannot be expected to reproduce the precise location of where fish come to land. It is also important to consider the length (Hemelrijk and Hildenbrandt, 2008) and maturity distribution within the schools themselves. In the current model, all particles are identical. Once biological information is included, we will be able to address such questions.

Using a bioenergetic model based on Dynamic Energy Budget (DEB) theory from ecology, we plan to explore the effect of maturation on the path of the spawning migration. The DEB model simulates the conversion of carbon uptake from food sources into body structure, internal reserves, and egg content of individuals over time (Gurney and Nisbet, 1998; Kooijman, 2000; Nisbet *et al.*, 2000). Incorporating this bioenergetic model into the simulations will allow us, for example, to change a fish's temperature preference and speed over time in response to the individual's energy reserves and sexual maturity. Such flexibility and individualization will enable us to modify the preferences for each fish as it matures, which we hope will aid us in reproducing the observed behavioural differences between varying age groups and sizes.

Acknowledgements

We are indebted to the Marine Research Institute (MRI) of Iceland for their support and for sharing their data and knowledge. The PhD thesis research of BE was funded by a grant from MRI, which also partially funded the PhD thesis research of AB. We are grateful too for the support from the Institute of Pure and Applied Mathematics at University College Los Angeles, as well as the Department of Mathematics at University College Santa Barbara. We also thank Hjálmar Vilhjálmsson for sharing his insight and helpful discussions and acknowledge the use of figures from his detailed book on the Icelandic capelin. Finally, we acknowledge the helpful comments from three anonymous referees.

References

Aoki, I. 1982. A simulation study on the schooling mechanism in fish. Bulletin of the Japanese Society of Scientific Fisheries, 48: 1081–1088.

Barbaro, A. B. T., Taylor, K., Trethewey, P., Youseff, L., and Birnir, B. Discrete and continuous models of the behavior of pelagic fish: applications to the capelin. Mathematics and Computers in Simulation, in press. doi:10.1016/j.matcom.2008.11.018.

Birnir, B. 2007. An ODE model of the motion of pelagic fish. Journal of Statistical Physics, 128: 535–568.

Buhl, J., Sumpter, D. J. T., Couzin, I. D., Hale, J. J., Despland, E., Miller, E. R., and Simpson, S. J. 2006. From disorder to order in marching locusts. Science, 312: 1402–1406.

Carscadden, J. E., Nakashima, B. S., and Frank, K. T. 1997. Effects of fish length and temperature on the timing of peak spawning in capelin (*Mallotus villosus*). Canadian Journal of Fisheries and Aquatic Sciences, 54: 781–787.

Chuang, Y. L., D'Orsogna, M. R., Marthaler, D., Bertozzi, A. L., and Chayes, L. S. 2007. State transitions and the continuum limit for a 2d interacting, self-propelled particle system. Physica D, 232: 33–47.

Couzin, I. D., Krause, J., James, R., Ruxton, G., and Franks, N. 2002. Collective memory and spatial sorting in animal groups. Journal of Theoretical Biology, 218: 1–11.

Czirók, A., Stanley, H. E., and Vicsek, T. 1997. Spontaneously ordered motion of self-propelled particles. Journal of Physics A, 30: 1375–1385.

Czirók, A., Vicsek, M., and Vicsek, T. 1999. Collective motion of organisms in three dimensions. Physica A, 264: 299–304.

Czirók, A., and Vicsek, T. 2000. Collective behaviour of interacting self-propelled particles. Physica A, 281: 17–29.

D'Orsogna, M. R., Chuang, Y. L., Bertozzi, A. L., and Chayes, L. S. 2006. Self-propelled particles with soft-core interactions: pattern, stability, and collapse. Physical Review Letters, 96: 104302.

Fiksen, Ø., Giske, J., and Slagstad, D. 1995. A spatially explicit fitness-based model of capelin migrations, the Barents Sea. Fisheries Oceanography, 4: 193–208.

Gjøsæter, H. 1998. The population biology and exploitation of capelin (*Mallotus villosus*) in the Barents Sea. Sarsia, 83: 453–496.

Gjøsæter, H., Dommasnes, A., and Røttingen, I. 1998. The Barents Sea capelin stock 1972–1997. A synthesis of results from acoustic surveys. Sarsia, 83: 497–510.

Grimm, V., Berger, U., Bastiansen, F., Eliassen, S., Ginot, V., Giske, J., Goss-Custard, D., *et al.* 2006. A standard protocol for describing individual-based and agent-based models. Ecological Modelling, 196: 359–374.

Grünbaum, D., Viscido, S., and Parrish, J. K. 2005. Extracting interactive control algorithms from group dynamics of schooling fish. *In* Cooperative Control: a Post-workshop Volume: 2003 Block Island Workshop on Cooperative Control. Lecture Notes in Control and Information Sciences, 309, pp. 103–117 Ed. by V. J. Kumar, N. E. Leonard, and A. S. Morse. Springer, Berlin.

Gurney, W. S. C., and Nisbet, R. M. 1998. Ecological Dynamics. Oxford University Press, New York.

Hemelrijk, C. K., and Hildenbrandt, H. 2008. Self-organized shape and frontal density of fish schools. Ethology, 114: 245–254.

Hemelrijk, C. K., and Kunz, H. 2005. Density distribution and size sorting in fish schools: an individual-based model. Behavioral Ecology, 16: 178–187.

Hubbard, S., Babak, P., Sigurðsson, S., and Magnússon, K. G. 2004. A model of the formation of fish schools and migration of fish. Ecological Modelling, 174: 359–374.

Huse, G. 2001. Modelling habitat choice in fish using adapted random walk. Sarsia, 86: 477–483.

Huse, G., Johansen, G. O., Bogstad, B., and Gjøsæter, H. 2004. Studying spatial and trophic interactions between capelin and cod using individual-based modelling. ICES Journal of Marine Science, 61: 1201–1213.

Huse, G., Strand, E., and Giske, J. 1999. Implementing behaviour in individual-based models using neural networks and genetic algorithms. Evolutionary Ecology, 13: 469–483.

Huth, A., and Wissel, C. 1992. The simulation of the movement of fish schools. Journal of Theoretical Biology, 156: 365–385.

Huth, A., and Wissel, C. 1994. The simulation of fish schools in comparison with experimental data. Ecological Modelling, 75: 135–146.

Kooijman, S. A. L. M. 2000. Dynamic Energy and Mass Budgets in Biological Systems. Cambridge University Press, Cambridge, UK.

Kunz, H., and Hemelrijk, C. K. 2003. Artificial fish schools: collective effects of school size, body size, and body form. Artificial Life, 9: 237–253.

Kunz, H., Züblin, T., and Hemelrijk, C. K. 2006. On prey grouping and predator confusion in artificial fish schools. *In* Proceedings of the Tenth International Conference of Artificial Life, pp. 365–371. Ed. by L. Mateus Rocha, L. S. Yaeger, M. A. Bedau, D. Floreano, R. L. Goldstone, and A. Vespignani. MIT Press, Cambridge, MA.

Magnússon, K., and Aspelund, T. 1997. A model for estimating meal frequency and meal size from stomach data with an application to Atlantic cod (*Gadus morhua*) feeding on capelin (*Mallotus villosus*). Canadian Journal of Fisheries and Aquatic Sciences, 54: 876–889.

Magnússon, K., and Pálsson, Ó. 1991. Predator–prey interactions of cod and capelin in Icelandic waters. ICES Marine Science Symposia, 193: 153–170.

Magnússon, K. G., Sigurðsson, S., Babak, P., Guðmundsson, S. F., and Dereksdóttir, E. H. 2004a. A continuous density Kolmogorov type model for a migrating fish stock. Discrete and Continuous Dynamical Systems, Series B, 4: 695–704.

Magnússon, K. G., Sigurðsson, S., and Dereksdóttir, E. H. 2005. A simulation model for capelin migrations in the North-Atlantic. Nonlinear Analysis: Real World Applications, 6: 747–771.

Magnússon, K. G., Sigurðsson, S., and Einarsson, B. 2004b. A discrete and stochastic simulation model for migration of fish with application to capelin in the seas around Iceland. Report RH-20-2004, Science Institute, University of Iceland.

Misund, O. A., Vilhjálmsson, H., Jákupsstofu, S. H., Røttingen, I., Belikov, S., Asthorsson, O., Blindheim, J., *et al.* 1998. Distribution, migration and abundance of Norwegian spring spawning herring in relation to the temperature and zooplankton biomass in the Norwegian Sea as recorded by coordinated surveys in spring and summer 1996. Sarsia, 83: 117–127.

Nisbet, R. M., Muller, E. B., Lika, K., and Kooijman, S. A. L. M. 2000. From molecules to ecosystems through dynamic energy budget models. Journal of Animal Ecology, 69: 913–926.

Partridge, B. L. 1982. The structure and function of fish schools. Scientific American, 246: 114–123.

Partridge, B. L., and Pitcher, T. J. 1980. The sensory basis of fish schools—relative roles of lateral line and vision. Journal of Comparative Physiology, 135: 315–325.

Reed, M., and Balchen, J. G. 1982. A multidimensional continuum model of fish population-dynamics and behaviour: application to the Barents Sea capelin (*Mallotus villosus*). Modeling Identification and Control, 3 : 65–109.

Sigurðsson, S., Magnússon, K. G., Babak, P., Guðmundsson, S. F., and Dereksdóttir, E. H. 2002. Dynamic continuous model of fish migration. Report RH-25-2002, Science Institute, University of Iceland.

Topaz, C. M., Bertozzi, A. L., and Lewis, M. A. 2006. A nonlocal continuum model for biological aggregation. Bulletin of Mathematical Biology, 68: 1601–1623.

Vicsek, T., Czirók, A., Ben-Jacob, E., Cohen, I., and Shochet, O. 1995. Novel type of phase transition in a system of self-driven particles. Physical Review Letters, 75: 1226–1229.

Vilhjálmsson, H. 1994. The Icelandic capelin stock. Journal of the Marine Research Institute Reykjavik, XIII. 281 pp.

Vilhjálmsson, H. 2002. Capelin (*Mallotus villosus*) in the Iceland–East Greenland–Jan Mayen ecosystem. ICES Journal of Marine Science, 59: 870–883.

Vilhjálmsson, H., and Carscadden, J. E. 2002. Assessment surveys for capelin in the Iceland–East Greenland–Jan Mayen area, 1978–2001. ICES Journal of Marine Science, 59: 1096–1104.

Viscido, S. V., Parrish, J. K., and Grünbaum, D. 2004. Individual behavior and emergent properties of fish schools: a comparison of observation and theory. Marine Ecology Progress Series, 273: 239–249.

Viscido, S. V., Parrish, J. K., and Grünbaum, D. 2005. The effect of population size and number of influential neighbours on the emergent properties of fish schools. Ecological Modelling, 183: 347–363.

Youseff, L. M., Barbaro, A. B. T., Trethewey, P. F., Birnir, B., and Gilbert, J. 2008. Parallel modeling of fish interaction. IEEE 11th International Conference on Computational Science and Engineering. Sao Paolo, Brazil.

doi:10.1093/icesjms/fsp067